doi:10.1246/cl.2012.104

Published on the web December 30, 2011

A Facile Fabrication of VO_2(A) Micro-nanostructures with Controlled Shape and Its Electrochemical Behavior in Lithium Ion Batteries

Wanqun Zhang,[1,2] Lei Shi,*[1] Kaibin Tang,[1] and Yang Yu[1]
[1]*Hefei National Laboratory for Physical Sciences at Micro-scale, University of Science and Technology of China, Hefei, Anhui 230026, P. R. China*
[2]*Chemical Experimental Teaching Center, University of Science and Technology of China, Hefei, Anhui 230026, P. R. China*

(Received October 22, 2011; CL-111041; E-mail: wqz@ustc.edu.cn)

VO_2(A) micro-nanostructures have been synthesized via a facile hydrothermal method by hydrolysis of oxidovandium(2+) ethylene glycolate in malonic acid solution. The novel morphologies of VO_2(A) could be readily tuned by altering the concentrations of malonic acid and reaction temperature. It is revealed that malonic acid played an important role as a structure directing agent helping the alternative formation of VO_2(A). Furthermore, their electrochemical properties were investigated, which reveal that the as-prepared VO_2(A) nanorods exhibit a relatively higher first discharge capacity than other VO_2(A) morphologies.

Vanadium oxides represent particularly attractive systems for such investigations because of their tremendous structural diversity arising from the facile accessibility of different vanadium oxidation states and their high tolerance for point defects.[1–4] Vanadium oxides exist mainly in five crystal phases: VO_2(R), VO_2(M), VO_2(B), VO_2(A), and recently reported VO_2(C). In particular, a great deal of attention has been paid to rutile type VO_2(R).[5,6] VO_2(R) is an iconic material which undergoes a Mott metal–insulator transition at a temperature of 68 °C in the bulk.[7] As a result, vanadium oxide has been proposed as a suitable material for constructing thermochromic devices and Mott field-effect transistors.[8–10] In contrast to VO_2(R), VO_2(A) has attracted less attention. The presence of VO_2(A) phase was first reported via a solid-state reaction in 1977.[11] However, the crystal structure of VO_2(A) had not been clarified until Oka and Yao, et al.[12,13] studied the structures of low-temperature and high-temperature VO_2(A) phases, respectively.

So far, several successful synthetic strategies have been demonstrated for the preparation of VO_2(A) materials via hydrothermal method.[14,15] However, they should be carried out under some special conditions, such as at relatively high temperature and for long reaction time. Moreover, shape-controlled VO_2(A) synthesis still remains challenging to chemists and material researchers. Thus, it is necessary to develop more facile, mild, and easily controlled methods to synthesize the shape-controlled VO_2(A) micro-nanostructures.

Herein, VO_2(A) was successfully prepared via a simple one-step hydrothermal method by hydrolysis of oxidovandium(2+) ethylene glycolate (VEG). The controlled crystal structures and morphologies were carried out for the first time to the best of our knowledge. In addition, among the various known vanadium oxides, a metastable oxide designated as VO_2(B), V_6O_{13}, and V_2O_5 have been found to show interesting cathode properties in lithium cells. The structures of VO_2(A) and VO_2(B) all consist of three-dimensional frameworks of VO_6 octahedra. In this study, VO_2(A) sharing a similar crystal structure with VO_2(B) was considered as a potential cathode material in lithium ion batteries.

All the reagents were of analytical grade and purchased from Shanghai Chemical, which were used as received without further purification. VEG was prepared according to the literature.[16] VEG (0.15 g) and malonic acid (1.2 g) were added into a 65-mL Teflon-lined stainless-steel autoclave, which was then filled with deionized water (45 mL). After stirring for 0.5 h, the autoclave was maintained at 180 °C for 12 h and cooled down to room temperature on standing. The products were collected and washed with distilled water, rinsed with ethanol, and then vacuum dried before characterization.

The products were characterized by X-ray powder diffraction (XRD) by using a Philips X-pert X-ray diffractometer with Cu Kα radiation ($\lambda = 1.54187$ Å). Scanning electron microscopy (SEM) images were taken with a Hitachi S-4800 scanning electron microanalyzer. The Brunauer–Emmett–Teller (BET) surface areas were measured with a Micromeritics ASAP 2000 system.

Figure 1 showed the XRD patterns of samples prepared under different conditions. Pure single-crystal tetragonal VO_2(A) phase could be obtained with control of experimental conditions which mainly included temperature and the concentrations of malonic acid (Figures 1b–1e). The XRD pattern of the synthetic product matches well that of ref 13, corresponding to the low-temperature, tetragonal form of VO_2(A) with space group $P4/$

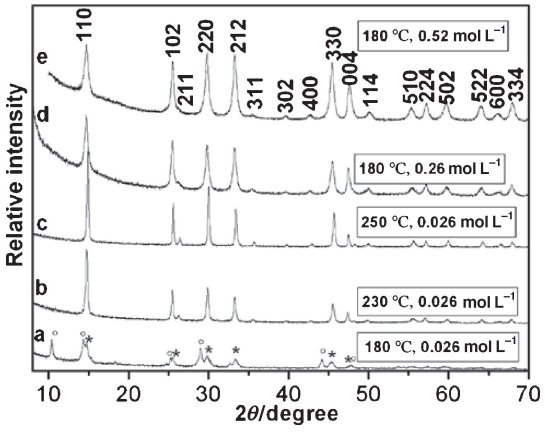

Figure 1. XRD patterns of the samples prepared with different concentrations of malonic acid at different reaction temperature for 12 h. The diffraction peaks corresponding to $H_2V_3O_8$ and VO_2(A) are marked with "○" and "∗," respectively.

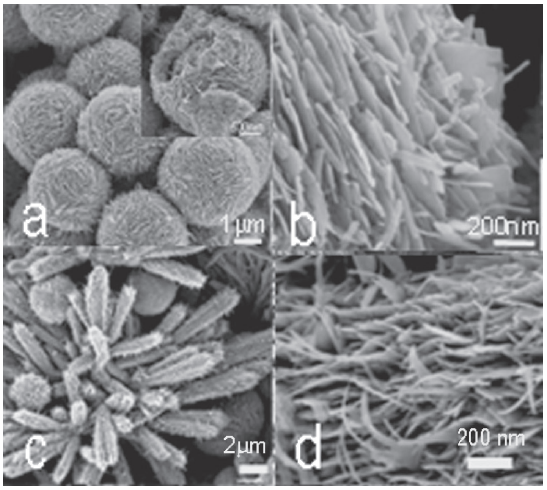

Figure 2. SEM images of VO_2(A) nanostructures synthesized with the different concentrations of malonic acid at 180 °C for 12 h: (a, b) 0.26 and (c, d) 0.52 mol L^{-1}.

ncc. It was found that lower concentrations of malonic acid or temperature taken in the hydrothermal treatment process would lead to the formation of a mixture of orthorhombic crystalline phase $H_2V_3O_8$ (JCPDS 852401) and VO_2(A) (Figure 1a). This result confirmed once more that the VO_2(A) is a metastable phase in vanadium dioxide, and its formation is very sensitive to preparing conditions.

The influences of the concentrations of malonic acid on the morphologies of VO_2(A) nanostructures have been investigated. Figures 2a and 2b present typical SEM images of VO_2(A) synthesized with 0.26 mol L^{-1} malonic acid at 180 °C for 12 h, revealing that the sample consists of uniform microspheres with an average diameter of 3 μm (Figure 2a). Figure 2a shows that the microspheres are flower-like and exhibit a hierarchical structure. The detailed morphology of the as-synthesized products is shown in Figure 2b, which clearly displays that the flower-like VO_2(A) microspheres are built from nanosheets on the surface. These nanosheets with a thickness of about 16 nm are connected to each other to form flower-like VO_2(A) microspheres. To reveal the inner structure of the microspheres, the broken microsphere provided an opportunity to investigate its morphology. The inset in Figure 2a shows a typical SEM image of the cross section of a broken microsphere, which reveals that the microsphere is composed of a VO_2(A) particle core, an outer particle layer, and a VO_2(A) nanosheet array on the outer particle layer. When the concentration of malonic acid was increased to 0.52 mol L^{-1}, as shown in Figures 2c and 2d, it is interesting to note that the cactus-like microcrystals began to appear with the increase of concentration. The cactus-like microcrystals usually consist of many branches with length between 5 and 12 μm growing out from the center (Figure 2c). The high-magnification SEM image of the single branch reveals that the branch nanostructures consist of many VO_2(A) nanosheets with thicknesses of 10–15 nm (Figure 2d). The nanosheets are very closely aligned along the axis of the branch.

Meanwhile, the reaction temperature is another vital factor in the formation of the morphology of the VO_2(A) structures. As the hydrothermal temperature was decreased to 150 °C, VO_2(A) was not obtained even if the concentration of malonic acid increased to 0.52 mol L^{-1} and reaction time extended to 72 h. When the hydrothermal temperature was increased to 180 °C and the concentrations of malonic acid is 0.026 mol L^{-1}, the mixture of $H_2V_3O_8$ and VO_2(A) was obtained (Figure 1a), confirming that the temperature is a critical factor for the formation of VO_2(A). When hydrothermal temperature was increased to 230 °C while the other conditions remained unchanged, as shown in Figures 3a and 3b, the as-prepared products include a large quantity of micrometer-sized arrays. Interestingly, the arrays consisted of nanorods that were aligned parallel to each other in micrometer-sized rods (Figure 3b). The length of the nanorods varies from 200 nm to 1 μm and their width from 30 to 60 nm. Figures 3c and 3d show typical SEM images of VO_2(A) nanostructures synthesized with 0.026 mol L^{-1} malonic acid at 250 °C. This SEM image (Figure 3c) clearly manifests the product is all nanorod morphology. High-magnification SEM images, as shown in Figure 3d, have further revealed that the nanorods have a smooth surface and a similar quadrangular cross section, with width and length of 50–100 nm and 1–3 μm, respectively. Furthermore, the image of as-prepared VO_2(A) indicates an obvious tendency for these nanorods to agglomerate.

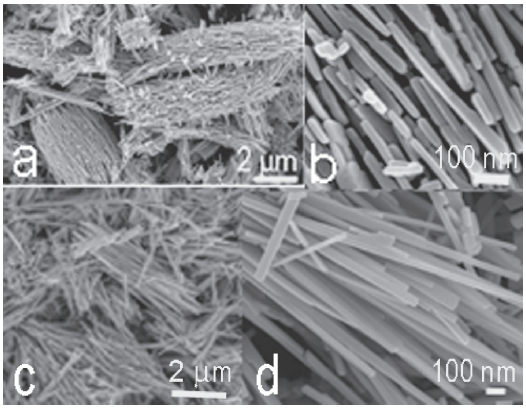

Figure 3. SEM images of VO_2(A) nanostructures synthesized with 0.026 mol L^{-1} concentrations of malonic acid at different temperature for 12 h: (a, b) 230 and (c, d) 250 °C.

It is well known that the $VO(OCH_2CH_2O)$ (VEG) structure is composed of one-dimensional chains. The chain contains edge sharing VO_5 square pyramids, whose oxygens come from a oxidovandium group (V=O), a chelating (–OCH_2CH_2O–) ligand and one end of two other (–OCH_2CH_2O–) ligands. The valence state of V ion in VEG is +4.[16] The reaction in the present system first yields VO^{2+} on hydrolysis in acidic conditions, and the following condensation of the VO^{2+} forms crystalline VO_2(A). The chemical reactions are proposed as follows:

$$VO(OCH_2CH_2O) + H_2O \xrightarrow{H^+} VO_2(A) + HOCH_2CH_2OH \quad (1)$$

It should be noted that malonic acid is necessary for the formation of VO_2(A). When only VEG was used for the precipitate formation at 250 °C for 24 h without malonic acid, VO_2(B) was obtained. To understand the role of malonic acid on the formation of VO_2(A), the experiments were carried out using oxalic acid or succinic acid instead of malonic acid as reaction

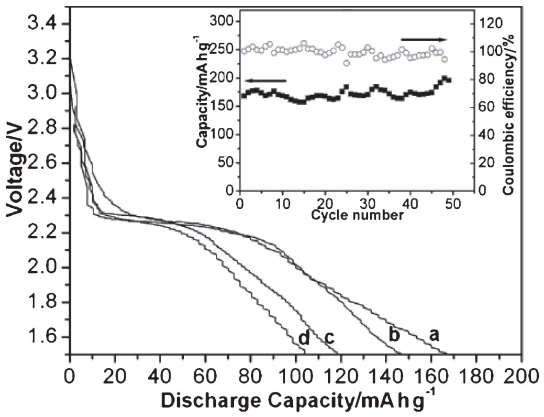

Figure 4. The first run discharge curves of our micro-/nano-VO_2 (A) at 50 mA g^{-1} at room temperature: (a) VO_2(A) nanorods, (b) micrometer-sized VO_2(A) arrays, (c) flower-like VO_2(A) microspheres, (d) the mixture of cactus-like VO_2(A) microcrystals and flower-like VO_2(A) microspheres. Inset: the capacity retention (square symbols) and Coulombic efficiency (circle symbols) as a function of cycle number of the as-prepared VO_2(A) nanorods.

medium, while the other parameters were kept constant. In consequence, VO_2(B) formed exclusively without any VO_2(A). We suspect that malonic acid played an important role as a coordinating ligand helping the formation of VO_2(A). It is supposed that malonic acid acts as a structure-directing agent for the formation of VO_2(A). In addition, in comparison with previously reported methods,[14,15] introduction of malonic acid not only is needed for synthesis of VO_2(A) but also has an advantage of shorter reaction time and lower reaction temperature. Furthermore, malonic acid can also act as a bidendate ligand able to modify the surfaces of growing nanocrystals, particularly the surface that possesses the lower electronic density, thus avoiding specific surface growth and providing the observed morphology difference when adjusting the malonate counter ion concentration.

VO_2(A) has been studied as cathode material for lithium ion batteries. Figure 4 shows the first run discharge curves of the as-prepared VO_2(A) cycled between 1.5 and 3.5 V at a current density of 50 mA g^{-1}. In the charge–discharge profiles, a distinct plateau at around 2.3 V can be observed. The as-prepared VO_2(A) nanorods demonstrated the reversible capacity is 166.7 mA h g^{-1} (Figure 4a). Meanwhile, the reversible discharge capacity for micrometer-sized VO_2(A) arrays, the flower-like VO_2(A) microspheres, and the mixture of cactus-like VO_2(A) microcrystals and flower-like VO_2(A) microspheres is 147.5 (Figure 4b), 118.4 (Figure 4c), and 106.5 mA h g^{-1} (Figure 4d), respectively. The BET surface areas of the as-prepared flower-like VO_2(A) microspheres, cactus-like VO_2(A) microcrystals, micrometer-sized VO_2(A) arrays, and VO_2(A) nanorods are 31.9, 33.1, 15.2, and 12.06 m^2 g^{-1}, respectively. To our knowledge, the morphology seems to be crucial to understanding the electrochemical performance.[17,18] In our experiment, the different electrochemical properties may mainly pertain to the crystallinity quality and size of the nanomaterials. The discharge specific capacities are plotted against cycle number on the as-prepared VO_2(A) nanorods, as shown in the inset in Figure 4. From the inset in Figure 4, the capacity of nanorods remained about 167 mA h g^{-1} at room temperature, which is slightly higher than that of VO_2(B) nanowires (140 mA h g^{-1}) at the same rate.[19] Moreover, there are no indication of a obvious capacity fade. According to the inset in Figure 4, it is obvious that the sample has a perfect cycling performance with a Coulombic efficiency of around 100%. On account of the effects of multifactors in electrical measurements, detailed research on the as-prepared VO_2(A) nanostructure will be done in our later work.

In summary, we have demonstrated a simple chemical route to the large-scale synthesis of low-valent VO_2(A) nanostructures. The difference in the concentration of malonic acid and temperature can be easily used to control the crystal morphology, such as flower-like VO_2(A) microspheres, cactus-like VO_2(A) microcrystals, micrometer-sized VO_2(A) arrays, and VO_2(A) nanorods. Malonic acid, as a structure directing agent, plays a very important role in an alternative preparation of the VO_2(A), which may be of much significance in the alternative synthesis of other low-valent vanadium oxide. Furthermore, electrochemical behavior of the as-prepared VO_2(A) has been reported. VO_2(A) nanorods deliver a higher capacity to store charge than other structures of VO_2(A) cycled under the same conditions, which mainly depends on the crystallinity and size.

This project was financially supported by the National Basic Research Program of China (973 program, Grant No. 2009CB939901), and the National Science Foundation of China, Grant No. 10874161.

References

1 M. Law, J. Goldberger, P. Yang, *Annu. Rev. Mater. Res.* **2004**, *34*, 83.
2 S. Surnev, M. G. Ramsey, F. P. Netzer, *Prog. Surf. Sci.* **2003**, *73*, 117.
3 R. Lopez, T. E. Haynes, L. A. Boatner, L. C. Feldman, R. F. Haglund, Jr., *Phys. Rev. B* **2002**, *65*, 224113.
4 Y. Wang, G. Cao, *Chem. Mater.* **2006**, *18*, 2787.
5 V. Eyert, *Ann. Phys. (Weinheim, Ger.)* **2002**, *11*, 650.
6 S. Biermann, A. Poteryaev, A. I. Lichtenstein, A. Georges, *Phys. Rev. Lett.* **2005**, *94*, 026404.
7 F. J. Morin, *Phys. Rev. Lett.* **1959**, *3*, 34.
8 J. C. Rakotoniaina, R. Mokrani-Tamellin, J. R. Gavarri, G. Vacquier, A. Casalot, G. Calvarin, *J. Solid State Chem.* **1993**, *103*, 81.
9 C. B. Greenberg, *Thin Solid Films* **1994**, *251*, 81.
10 H.-T. Kim, B.-G. Chae, D.-H. Youn, S.-L. Maeng, G. Kim, K.-Y. Kang, Y.-S. Lim, *New J. Phys.* **2004**, *6*, 52.
11 F. Théobald, *J. Less-Common Met.* **1977**, *53*, 55.
12 T. Yao, Y. Oka, N. Yamamoto, *J. Solid State Chem.* **1994**, *112*, 196.
13 Y. Oka, S. Sato, T. Yao, N. Yamamoto, *J. Solid State Chem.* **1998**, *141*, 594.
14 S. Ji, Y. Zhao, F. Zhang, P. Jin, *J. Ceram. Soc. Jpn.* **2010**, *118*, 867.
15 S. Zhang, B. Shang, J. Yang, W. Yan, S. Wei, Y. Xie, *Phys. Chem. Chem. Phys.* **2011**, *13*, 15873.
16 P. Ragupathy, S. Shivakumara, H. N. Vasan, N. Munichandraiah, *J. Phys. Chem. C* **2008**, *112*, 16700.
17 D. K. Kim, P. Muralidharan, H.-W. Lee, R. Ruffo, Y. Yang, C. K. Chan, H. Peng, R. A. Huggins, Y. Cui, *Nano Lett.* **2008**, *8*, 3948.
18 X. Xiao, L. Wang, D. Wang, X. He, Q. Peng, Y. Li, *Nano Res.* **2009**, *2*, 923.
19 G. Armstrong, J. Canales, A. R. Armstrong, P. G. Bruce, *J. Power Sources* **2008**, *178*, 723.

